

# Recycling of porcelain stoneware scraps in alkali bonded ceramic composites

Valentina Medri, Elena Landi\*

*CNR-ISTEC, National Research Council of Italy, Institute of Science and Technology for Ceramics, via Granarolo, 64, I-48018 Faenza, Italy*

Received 6 February 2013; received in revised form 23 May 2013; accepted 1 June 2013

Available online 15 June 2013

## Abstract

Ground porcelain stoneware scraps have been recycled as a partially reactive filler in alkali bonded ceramic composites. Sandwich panels were prepared by varying the dimension and amount of scraps in the core and skins. The alkali bonding was realized by using highly reactive metakaolin powder and alkaline  $\text{KOH}/\text{K}_2\text{SiO}_3$  aqueous solution. The setting was performed at  $80^\circ\text{C}$  for 24 h. The thermal conductivity of the panels at room temperature was  $0.7\text{ W m}^{-1}\text{ K}^{-1}$ . Investigations on the extent of capillary water absorption and water release indicated the possibility to exploit the water retention properties of the binder for cooling by water evaporation.

© 2013 Elsevier Ltd and Techna Group S.r.l. All rights reserved.

**Keywords:** C. Thermal conductivity; Porcelain stoneware; Geopolymers; Microstructure

## 1. Introduction

With an ever increasing environmental awareness, industrial waste recycling is becoming a priority. Many industrial ceramic and glass wastes could be reused to produce construction and refractory materials [1,2].

The wall and floor ceramic tile industry produces a large amount of waste such as polishing sludge as well as discarded tiles. Regardless of the kind of product being manufactured, the starting mix for traditional ceramic must include three types of materials: a plastic material (clay), a fluxing agent to facilitate melting (such as feldspars, nepheline, etc.) and a non-plastic material to provide structural strength (such as sand and chamotte). Chamotte is a porcelain material made from recycled tiles that are wet ground and milled as scraps. However, the quantity of chamotte required by industrial processes is well below the total amount of waste tiles produced, which must necessarily end up in a landfill, with the consequent high costs of transportation and disposal.

The possibility to recycle residue coming from the industrial polishing process of porcelain stoneware tiles by using it in a porcelain stoneware body mix was studied by Rambaldi et al. [3]. Moreover, scraps from porcelain stoneware tiles can be used as fillers and aggregates to limit shrinkage and add mechanical strength to hydraulic cement systems, such as Portland cement concrete [1]. An example of the use of fired ware scraps, another type of ceramic waste material from the automobile industry, in Portland cement concrete (PCC) and hot-mix asphalt (HMA) has been evaluated by Huang et al. [4] with the purpose of replacing fine aggregates in paving material.

In addition to hydraulic cements, alkali-aluminosilicate binders, the so called geopolymers [5], are proving to be promising inorganic alternatives to organic matrices for the preparation of composite materials. They belong to the alkali bonded ceramics category, i.e. materials obtained from the reaction of an aluminosilicate powder, such as coal fly ash, calcined clay and/or metallurgical slag, with a highly concentrated alkali hydroxide solution ( $\text{KOH}$ ,  $\text{NaOH}$ ) and/or with alkaline silicate ( $\text{KSi}_2\text{O}_3$  or  $\text{NaSi}_2\text{O}_3$ ) solution, which leads to the formation of a synthetic alkali-aluminosilicate. Unlike calcium-based cements (such as Portland cements), geopolymers do not take in hydration water within the crystal structure

\*Corresponding author. Present address: CNR-ISTEC, Via Granarolo 64, 48018 Faenza, Italy. Tel.: +39 0546699757; fax: +39 054646381.

E-mail address: [elena.landini@istec.cnr.it](mailto:elena.landini@istec.cnr.it) (E. Landi).

and, although they are processed at temperatures below 120 °C, they can resist up to 1200 °C, depending on their composition [5]. Today the primary application of geopolymer technology is in the development of reduced-CO<sub>2</sub> construction materials as an alternative to ordinary Portland cements.

Geopolymer matrices consist of nano-precipitates [6,7] that may act as a binder for introduced fillers (glass, ceramic, metal or organic powders or fibres) forming a composite material. Obviously, different fillers can be used to tailor specific physical and thermo-mechanical properties, depending on the applications for which the alkali bonded composites are designed [8–12].

In this study, alkali bonded ceramic composites were used to produce panels with a sandwich structure for thermal insulation and passive cooling, following the idea of an eco-efficient process:

1. by recycling in the composition up to 80 wt% of porcelain stoneware scraps with different granulometry from discarded tiles (manufactured in the ceramic districts of Sassuolo-Scandiano Emilia Romagna, Italy);
2. by using a synthetic alkali-aluminosilicate as a chemically active binder (which allows chemical consolidation at low temperature), to avoid resorting to high temperatures (typically used in ceramic consolidation) during the production process of the panel and to exploit the water retention properties of the geopolymer for cooling by water evaporation [13].

This low temperature production process reduces the impact on the environment by reusing scraps, that would otherwise be dumped in a landfill. The use of ceramic waste also offers benefits in terms of recovering the energy previously stored during their production. In fact ceramic factory wastes, regardless of the reason for which they have been discarded (breakage-deformation or over- or under- firing defects) are “fired clay”, which means that they have been thermally activated (900–1200 °C) during the manufacturing process. Therefore different rejects with different chemical and mineralogical compositions might have similar reactive properties. Moreover, in fired porcelain stoneware, crystalline phases such as mullite, quartz and feldspars are embedded in a glassy matrix having a quartz-feldspathic composition that ranges between 40 and 75 wt% [14]. The alumino-silicatic glassy phase is more likely to dissolve into an alkaline solution than

the embedded crystalline phases, and porcelain stoneware scraps may play the role of partially reactive fillers. Indeed, the glassy nature of both fly ashes and ground granulated blast furnace slags are the reason for the high geopolymer reactivity of these industrial wastes [5].

Finally, the panels being presented here could be cast and cured directly at the ceramic district site, since the required raw materials (such as kaolin, metakaolin and alkali silicates) are commonly used by the ceramic tile industry, thus reducing transportation costs. The presence of ceramic production and waste recycling sites in the same location would hence consolidate the peculiar and typical features of the ceramic industry sector that has grown and is still developing around specific “clusters”, where companies working in the same or related sectors are located in the same geographical area.

## 2. Experimental

### 2.1. Binder and scrap-based composites preparation

The alkali-aluminosilicate binder was prepared by using metakaolin as raw powder. Metakaolin was prepared by calcining commercial kaolin (BS4, AGS Mineraux, Clèrac, France) at 750 °C for 15 h in an electric kiln. The main characteristics of the BS4 kaolin source for the metakaolin raw powder are reported elsewhere [15].

Potassium silicate solutions with a SiO<sub>2</sub>:K<sub>2</sub>O molar ratio equal to 2.00 and a H<sub>2</sub>O:K<sub>2</sub>O molar ratio equal to 23.00 were prepared by dissolving KOH pellets (purity > 99%, Merck, Germany) into a potassium silicate aqueous solution with a SiO<sub>2</sub>:K<sub>2</sub>O molar ratio equal to 3.57 (KSil 35Bè R3.5, Ingessil, Italy) by magnetic stirring. Geopolymer with SiO<sub>2</sub>:Al<sub>2</sub>O<sub>3</sub> molar ratio equal to 4.00 was prepared by mixing metakaolin with the KOH/K<sub>2</sub>SiO<sub>3</sub> aqueous solution mechanically for 2 min at 100 r.p.m. The resulting slurry was then placed in plastic moulds and cured in a heater at 80 °C for 24 h.

Two grades of ground porcelain stoneware scraps (Fig. 1) were used as filler:

- S1- humidity: 2.99%; granulometry: > 5 mm = 2.52%; 2–5 mm = 39.50%; 1–2 mm = 23.72%; 400 µm–1 mm = 16.88%; < 400 µm = 17.38%.

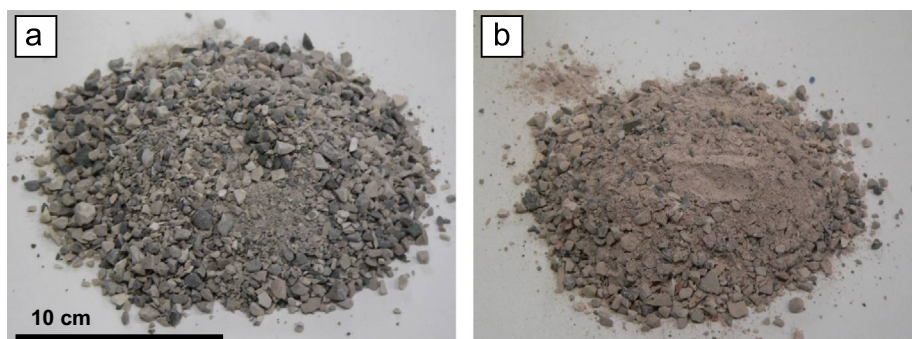


Fig. 1. Ground porcelain stoneware scraps S1 (a) and S2 (b).

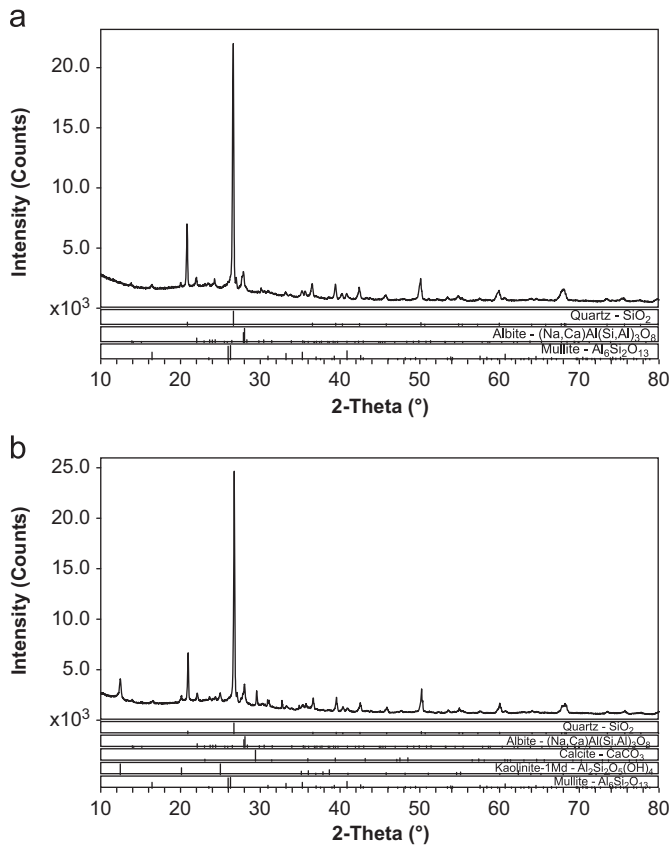


Fig. 2. XRD spectra of ground porcelain stoneware scraps S1 (a) and S2 (b).

- S2- humidity:0.08%; granulometry: > 5 mm=1.40%; 2–5 mm=41.84%; 1–2 mm=21.04%; 400  $\mu$ m–1 mm=12.74%; < 400  $\mu$ m=22.98%.

S1 consisted entirely of post firing process (about 1200 °C) ground porcelain stoneware because it is composed by crystalline phases such as mullite, quartz and feldspar (Fig. 2a). The estimated amount of glassy phase is 63 wt%. In S2, the coarse fraction consisted of fired porcelain stoneware tiles (chamotte), while the < 400  $\mu$ m fraction is mainly made up of pre-firing porcelain stoneware, as kaolinite and calcite were still present (Fig. 2b). Considering the composition range of different porcelain stoneware products [14], both S1 and S2 scrap compositions can be considered representative of this kind of material. These materials are classified as non-hazardous, in the European List of Waste, with code 101208- ceramic brick, roof tile and construction material wastes (fired).

Scraps were mechanically mixed at 100 r.p.m for 2 min at room temperature into the binder slurry. Scrap amounts were varied to produce different compositions for the sandwich core and skin. The resulting composite pastes were poured into plastic moulds and cured in a heater at 80 °C for 24 h.

The sandwich panels were produced by pouring sequentially into the mould the specifically formulated pastes for skin–core–skin.

## 2.2. Characterisation

BET analyses were performed using SORPTY 1750, Carlo Erba Instruments, Milan, Italy. Pore size distribution in the range 0.0037–58  $\mu$ m was analysed by mercury porosimetry (Thermo Finnigan Pascal 140 and Thermo Finnigan Pascal 240, Milano, Italy). Real density was measured by Helium pycnometer 1305 Micromeritics, Peschiera, Italy.

Binder and scrap-based composite samples were examined by scanning electron microscopy equipped with X-ray microprobe (SEM, Cambridge S360, Cambridge, UK; EDS, INCA Energy 300, Oxford Instruments, Oxford, UK).

A Bruker D8 Advance diffractometer with CuK $\alpha$  radiation (Karlsruhe, Germany) was used to determine the crystalline phases.

The bulk density and porosity of the composites were determined by weight-to-volume ratio. The morphological and microstructural features were observed by SEM. Ultra-macro-porosity was investigated by image analysis (Image Pro Plus 6.0., Media Cybernetics, Inc. Bethesda, MD, USA) of high resolution photos (scanner Sharp JX330, Japan) and of scanning electron micrographs of the cross sections.

Thermal conductivity was measured on 30 cm  $\times$  30 cm  $\times$  5 cm sandwich panels by using a Guarded Hot Plate Apparatus. The Guarded Hot Plate Apparatus in accordance with ASTM C177-97 standard measures the steady-state heat flux through flat specimens of materials having a “low” thermal conductivity and commonly denoted as “thermal insulators”. Acceptable measurement accuracy requires a specimen geometry with a high area to thickness ratio.

Capillary absorption was determined according to UNI EN 772-11 (2011) on a 5 cm  $\times$  5 cm  $\times$  2.5 cm (height) sample constituted by the core and just one skin layer (0.5 cm thick). The sample was first dried in a heater at 100 °C and its mass ( $m_{dry,s}$ ) was measured after cooling. The skin surface ( $A_s$ ) was submerged at a depth of 5 mm, i.e. the whole skin thickness, in distilled water at 25 °C. The sample was held by thin holders in order to avoid any contact with the bottom of the vessel and to keep the main part of the surface in contact with the water. The test was performed in a closed vessel in order to reach saturation conditions. The water level was kept constant during the test. The specimen mass ( $m_{so,s}$ ) was recorded after 1 min ( $t$ ). Then, the sample was stored in a desiccator with controlled relative humidity, set at about 50% (25 °C) and the mass ( $m_{wr,ti}$ ) was measured at time  $t_i$  up to 48 h after the capillary absorption test.

The initial coefficient of capillary absorption of water ( $C_{wi,s}$ ) was calculated by the formula:

$$C_{wi,s} = (m_{so,s} - m_{dry,s}) / (A_s t) [\text{kg} / (\text{m}^2 \text{ min})] \quad (1)$$

The percentage of water absorption after 1 min was calculated as:

$$WA = (m_{so,s} - m_{dry,s}) / m_{dry,s} [\%] \quad (2)$$

The maximum percentage of absorbed water (WS) was reached when water saturation was measured after five days of complete submersion of the specimen in distilled water.

The percentage of water release at each time  $t_i$  was calculated as:

$$WR_i = (m_{wr,ti} - m_{so,s}) / m_{so,s} [\%], \quad (3)$$

and plotted versus time to determine the coefficient of water release ( $C_{WR}$ ) as the slope of the plot.

### 3. Results and discussion

#### 3.1. Alkali-aluminosilicate binder and binding effects on scraps

The high specific surface area of the metakaolin used ( $30 \text{ g/cm}^3$ , [15]) suggests a potentially high reactivity during the initial dissolution process of geopolymerization, since the metakaolin reactivity is not even and depends on both its morphology and degree of dehydroxylation, and may result in a different degree of geopolymerization [5,16].

SEM micrographs of the fracture surfaces of the synthetic alkali-aluminosilicate after setting are reported in Fig. 3 to highlight the microstructure at different scale ranges. Micrometric porous structures (Fig. 3a) were formed by flakes of agglomerated nano-precipitates of about 60 nm (Fig. 3b). The specific surface area and the bulk density of the alkali-aluminosilicate binder were  $3.2 \text{ m}^2/\text{g}$  and  $2.26 \pm 0.01 \text{ g/cm}^3$ , respectively.

The dimension of the nano-particles was higher and the specific surface area was lower than the values reported in literature ( $30\text{--}130 \text{ g/cm}^3$  [17]) because of the higher dilution of the  $\text{KOH}/\text{K}_2\text{SiO}_3$  aqueous solution (molar ratio  $\text{H}_2\text{O}/\text{K}_2\text{O}=23$  instead of 11 [17]). Water does not enter into the geopolymer framework but behaves as a steric hindrance and acts as a pore agent upon its removal during setting at  $80^\circ\text{C}$  [13,18–20]. The total porosity of the geopolymer is 55% with an average pore diameter of  $1.09 \mu\text{m}$  (Fig. 4), confirming the results obtained by using another type of metakaolin as raw material [20].

In the composite material, nano-precipitates act as a binder for porcelain stoneware scraps (Fig. 5a, b). For comparison, the fractions with granulometry  $\leq 400 \mu\text{m}$  of both S1 and S2 scraps have been treated separately with the  $\text{KOH}/\text{K}_2\text{SiO}_3$  aqueous solution with the same process modalities of the binder and the panel. Geopolymer nano-precipitates formation is observed for both S1 (Fig. 5c) and S2 as well (Fig. 5d).

The XRD characterisation shown in Fig. 6a highlights the mainly amorphous nature of the alkali-aluminosilicate binder, with peaks due to quartz and illite which were already present in the metakaolin raw powder [15]. Conversely, the XRD spectrum of a composite (Fig. 6b) where the total amount of scraps is 57 wt% and the binder is stoichiometric (composition A in Table 1) showed an amorphous hump with crystalline peaks due to quartz (from metakaolin raw powder and scraps) and feldspar (from scraps). Crystalline phases do not have a tendency to take part in the geopolymerization process. According to Zibouche et al. [21], the presence of inert phases does not influence the geopolymerization reaction.

Kaolinite, which is found in S2 scraps, is a geopolymer source material, in spite of its scarce reactivity [22]. Porcelain stoneware tiles contain 40–75 wt% of a vitreous phase having a quartz-feldspathic composition with an alumina excess coming from clay mineral breakdown after firing [14]. The glassy phase contains about 70 wt% of non-crystalline  $\text{SiO}_2$  and 20 wt% of  $\text{Al}_2\text{O}_3$  [14]. S1 scraps contain 63 wt% of amorphous phase. This amorphous phase partially dissolves in alkaline media, such as  $\text{KOH}/\text{K}_2\text{SiO}_3$  aqueous solution (pH about 12) at  $80^\circ\text{C}$ , especially regarding its silica content. Hydroxyl anion ( $\text{OH}^-$ ) is considered to be a catalyst for the dissolution reaction of silica [23]. Silica is an acidic oxide and

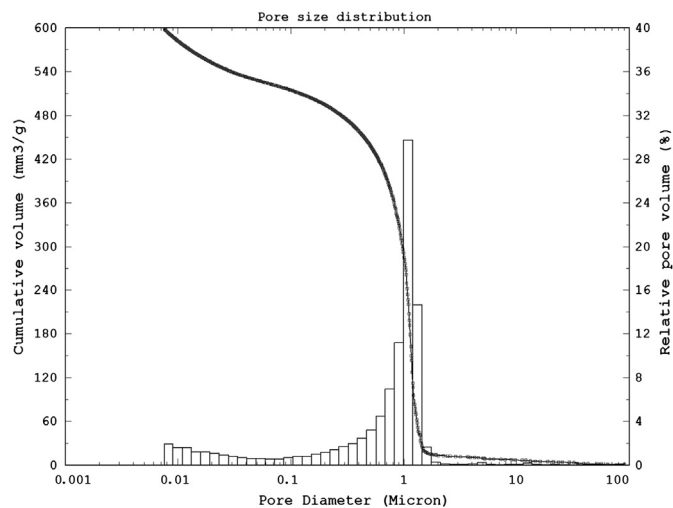


Fig. 4. Pore size distribution of the geopolymer after setting.

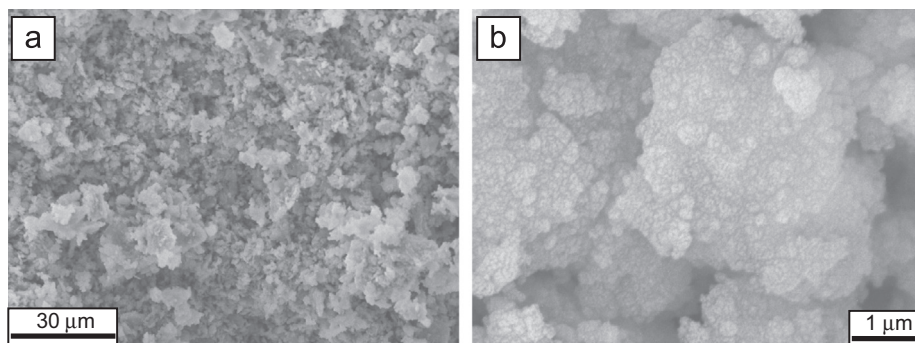


Fig. 3. SEM micrographs of the fracture surfaces of the geopolymer after setting.



dissolves in alkaline media at  $\text{pH} > 11$ , and the dissolution increases with the temperature.  $\text{Al}_2\text{O}_3$  behaves similarly due to its amphoteric character. Due to the presence of glassy phase, nano-precipitates tend to form on the surface of the scraps (Fig. 5). Therefore porcelain stoneware scraps can be considered a partially reactive filler that promotes alkali-bonding with a surface reaction. The surface bonding related to the presence of amorphous phases such as silica was already observed when silicon carbide particles were used as filler [15,23,24–25].

### 3.2. Scrap-based composites and scale up to sandwich panels

Scrap amounts in the compositions were dosed differently to produce the core and skins. The relative amounts of raw

materials were determined through a trial-and-error approach due to the great variability in scrap granulometry and glassy phase in the blended scraps. A selection of the most suitable scrap-based composites for both core and skin is reported in Table 1 and shown in Fig. 7.

Compositions A and B (Table 1) were selected for skins. Composition A and the similar ones (not reported in Table 1) with a scrap amount  $< 60$  wt% had a stoichiometric amount of  $\text{KOH}/\text{K}_2\text{SiO}_3$  aqueous solution in respect with metakaolin. Thus the surface of the skin had the appearance of the highly porous binder resin with embedded scraps (Fig. 7).

Composition B was produced with an excess of  $\text{KOH}/\text{K}_2\text{SiO}_3$  aqueous solution in respect to metakaolin for the geopolymer binder. Because it is a liquid medium, excess of water glass allowed the incorporation of a higher percentage of

Table 1

Compositions and densities of the most suitable scrap-based composites for the core and skins of the sandwich panel.

|  | A                  | B                  | C                  | D                  | E                | F                | G                  | H                  | I                  | J                | K                | L                  | M                |
|--|--------------------|--------------------|--------------------|--------------------|------------------|------------------|--------------------|--------------------|--------------------|------------------|------------------|--------------------|------------------|
| Metakaolin wt%                                   | 14.3               | 7                  | 7.7                | 7.7                | 7.7              | 6.7              | 6.7                | 6.7                | 5.7                | 5.7              | 6.7              | 6.7                | 5.7              |
| $\text{KOH}/\text{K}_2\text{SiO}_3$ solution wt% | 28.7               | 21                 | 15.3               | 15.3               | 15.3             | 13.3             | 13.3               | 13.3               | 11.3               | 11.3             | 13.3             | 13.3               | 11.3             |
| S1 wt%   | 28.5               | 36                 | 38.5               | –                  | 77               | –                | 80                 | 40                 | 83                 | 41.5             | 13               | 26                 | 17               |
| S2 wt%   | 28.5               | 36                 | 38.5               | 77                 | –                | 80               | –                  | 40                 | –                  | 41.5             | 67               | 54                 | 66               |
| S total wt%                                      | 57                 | 72                 | 77                 | 77                 | 77               | 80               | 80                 | 80                 | 83                 | 83               | 80               | 80                 | 83               |
| Density ( $\text{g}/\text{cm}^3$ )               | 1.45<br>$\pm 0.06$ | 1.60<br>$\pm 0.04$ | 1.59<br>$\pm 0.09$ | 1.35<br>$\pm 0.07$ | 1.4<br>$\pm 0.1$ | 1.2<br>$\pm 0.1$ | 1.45<br>$\pm 0.09$ | 1.05<br>$\pm 0.08$ | 0.06<br>$\pm 0.07$ | 1.0<br>$\pm 0.1$ | 1.1<br>$\pm 0.1$ | 1.04<br>$\pm 0.05$ | 0.8<br>$\pm 0.1$ |

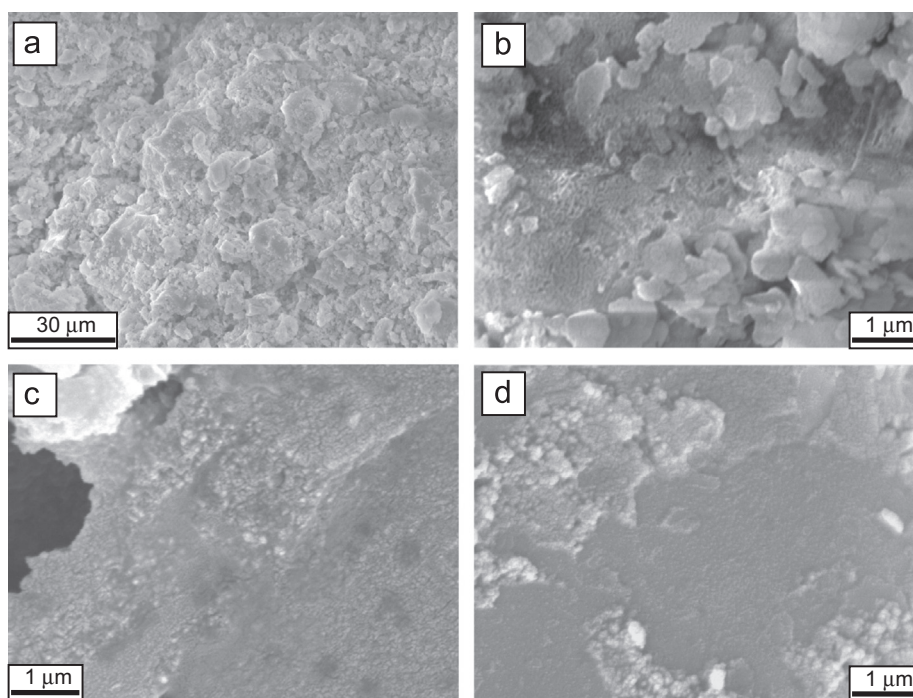


Fig. 5. SEM micrographs of the fracture surfaces of a porcelain stoneware scraps composite with alkali-aluminosilicate binder (a and b) and S1 (c) and S2 (d) scraps with granulometry  $\leq 400$   $\mu\text{m}$  bonded with the  $\text{KOH}/\text{K}_2\text{SiO}_3$  aqueous solution. Geopolymer nano-precipitates formation has been evidenced in all cases.

scraps (up to 72 wt%), it filled and closed the pores so as to maintain a flat and homogenous surface (detail in Fig. 7) compared to composition A. For this reason, composition B was chosen for skins although its density was higher than in composition A ( $1.45 \pm 0.06 \text{ g/cm}^3$  in A and  $1.60 \pm 0.04 \text{ g/cm}^3$  in B, Table 1).

Compositions C–M were studied for the purpose of producing the macro-porous core of the sandwich panels. They all contain a stoichiometric amount of alkaline solution, since the result is a highly porous binder. Millimetric sized granules are packed and stacked so that a network of interconnected voids forms between them creating the ultramicro-porous architecture.

Compositions C–E contained 77 wt% of scraps. A non-homogeneous sedimentation of the binder occurred on the bottom of the mould (Fig. 5). This sedimentation was particularly evident when only scraps S1 were used. These scraps are moistened and consequently the absorbed water contributed to decrease the binder viscosity and to increase scrap sedimentation.

Compositions F–M contained scraps up to 83 wt%. The scrap amount and grade were varied to reach a minimum density. The measured densities varied greatly due to different granule packing or inhomogeneous sampling of the scraps. When 83 wt% of scraps were used, granules tended to detach from the samples because the amount of binder was insufficient. Composition L (see detail in Fig. 7) was the most reliable and reproducible (Table 1).

In Fig. 8 the material scale up is shown: sample dimensions vary from  $5 \text{ cm} \times 5 \text{ cm} \times 2.5 \text{ cm}$  to  $15 \text{ cm} \times 15 \text{ cm} \times 3.5 \text{ cm}$  and finally a  $30 \text{ cm} \times 30 \text{ cm}$  sandwich panel was prepared with two 0.5 cm thick skins of composition B and a 4 cm thick core of composition L. The density of the final sandwich panel was about  $1100 \text{ kg/m}^3$ .

### 3.3. Thermal conductivity

The panel's thermal conductivity at room temperature was  $0.7 \text{ W m}^{-1} \text{ K}^{-1}$  (Table 2 and Fig. 9), thus being lower than the value ( $\sim 1.5 \text{ W m}^{-1} \text{ K}^{-1}$ , Garcia et al., [26]) characterising the original scrap material and laying in the range of values ( $0.4\text{--}0.8 \text{ W m}^{-1} \text{ K}^{-1}$ ) typical of geopolymers [27].

### 3.4. Capillary water absorption and water release

The data recorded for capillary water absorption and water release ability are reported in Table 2.

The initial coefficient of water absorption  $C_{\text{wis}}$  is  $2.4 \text{ kg/(m}^2 \text{ min)}$ . This value is much higher than the values ( $\sim 1 \times 10^{-2} \text{ kg/(m}^2 \text{ min)}$ ) reported in literature for the initial rate of water absorption of clay masonry units such as bricks [28].

The maximum percentage of water absorption at water saturation (after 5 days) WS is 9.2%. The water absorption percentage WA after 1 min is 6.9%, i.e. 75% of the value at water saturation. The plot of the water release percentage  $WR_i$  (formula 3) against time  $t_i$  is reported in Fig. 10. The water

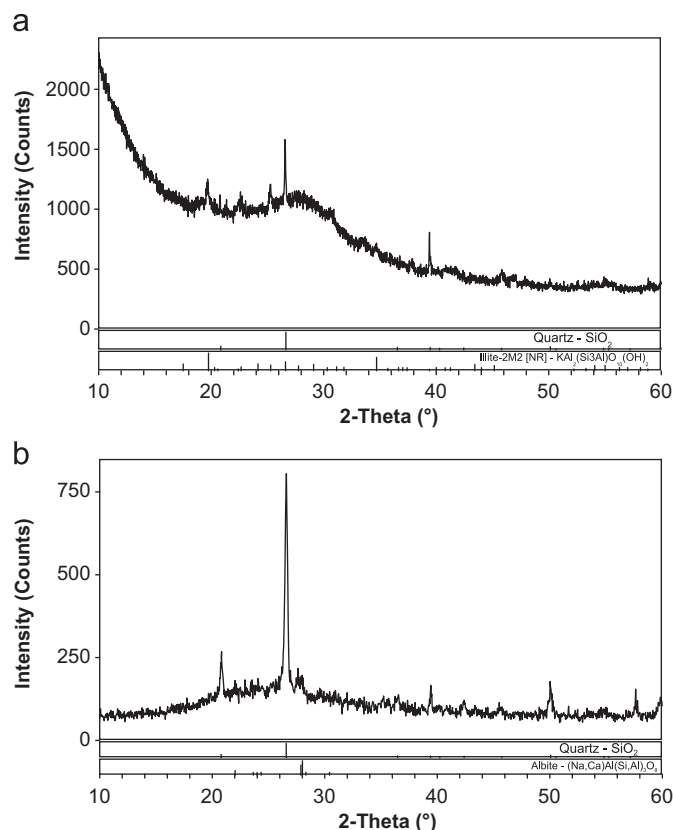


Fig. 6. XRD spectra of the synthetic alkali-aluminosilicate binder (a) and of a composite (b) where the total amount of scraps is 57 wt% and the binder is stoichiometric (composition A in Table 1).

release trend is exponential with time:

$$WR_i = 6.6084e^{-0.0426t_i} \quad (4)$$

By fitting the  $WR_i$  trend in the first 20 h according to a linear law, the coefficient of water release  $C_{\text{WRa}}$ , calculated as the slope of the plot, is about 0.2%/h. Considering the successive time period (20–50 h) the  $C_{\text{WRb}}$ , value decreases to about 0.07%/h.

Capillary water absorption depends on microstructural characteristics, especially pore amount, size and shape. Linear relationships between the capillary absorption and these microstructural variables in both clay bricks and geopolymers are already reported in literature [13,28], confirming the role of open porosity in increasing the material's water absorption. In particular, greater pore dimensions increase the water absorbing rate and, consequently, that of water release [13]. Accordingly, the geopolymer network that constitutes the binder in the composite sandwich panels has been produced by using a high molar ratio of  $\text{H}_2\text{O/K}_2\text{O} = 23$  where, as previously discussed, water acts as a pore agent forming, upon its removal during setting at  $80^\circ\text{C}$ , pores with a large average diameter (980 nm). The highly porous geopolymer network induces a fast water uptake that approaches saturation in 1 min (75% of the saturation level is reached). The water release ability determines the discharge of most of the absorbed water within 48 h, with release rates progressively decreasing with time.

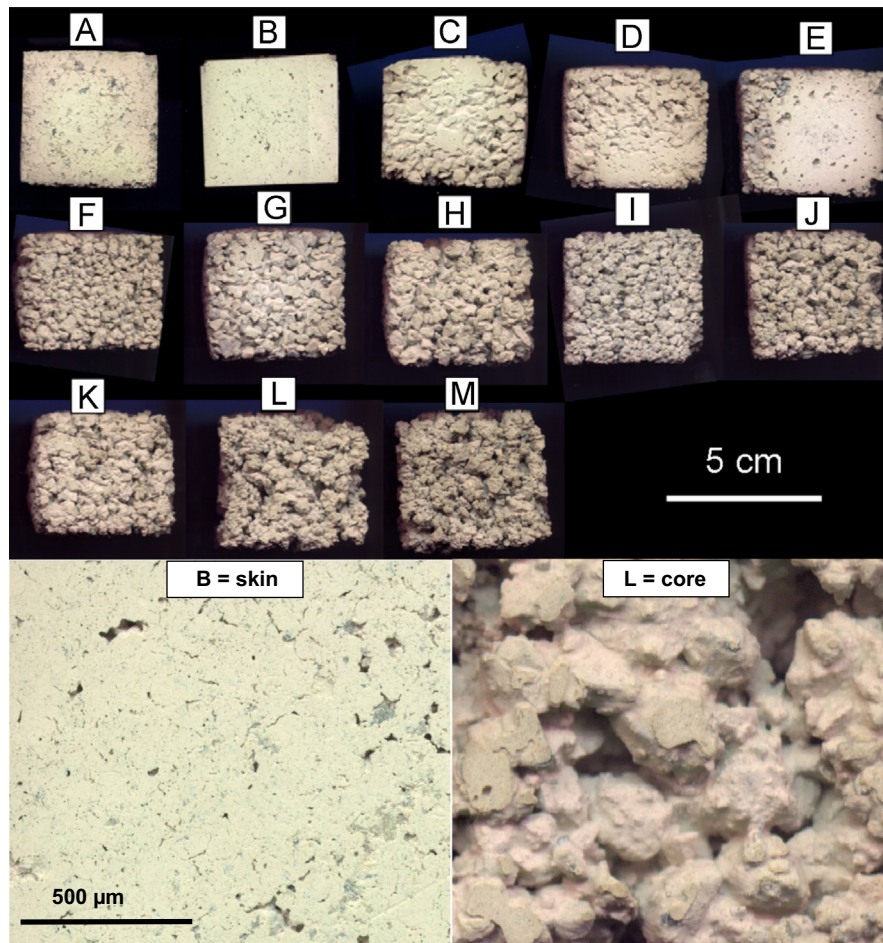


Fig. 7. High resolution photos of a selection of the most suitable scrap-based composites for both core and skin (see Table 1) and surface details of composition B and L selected respectively for skin and core of the sandwich panel.



Fig. 8. Pictures of the material scale up: sample dimensions vary from 5 cm × 5 cm × 2.5 cm (a) to 15 cm × 15 cm × 3.5 cm (b) and finally 30 cm × 30 cm sandwich panel (c) was prepared with 0.5 cm thick skins of composition B and 4 cm thick core of composition L (see Table 1).

It is necessary to point out that upon water saturation the composite sandwich panel shows a weight increase of only 9.2%, while in geopolymer binders the weight gain is up to

60% [13]. This low weight increase due to water absorption should hence contribute to avoid any excessive structural overload.



Table 2

Thermal conductivity  $\lambda$  at room temperature and capillary water absorption and water release data: initial water absorption coefficient  $C_{wis}$ , water absorption percentage WA, water release coefficient  $C_{WRa}$  in the first 20 h, water release coefficient  $C_{WRb}$  in the following time period (20–50 h).

| $C_{wis}$ , kg/(m <sup>2</sup> min) | WA, % | WS, % | $C_{WRa}$ , %/h | $C_{WRb}$ , %/h | $\lambda$ , W m <sup>-1</sup> K <sup>-1</sup> |
|-------------------------------------|-------|-------|-----------------|-----------------|---|
| 2.4                                 | 6.9   | 9.2   | 0.2             | 0.07            | 0.7   |

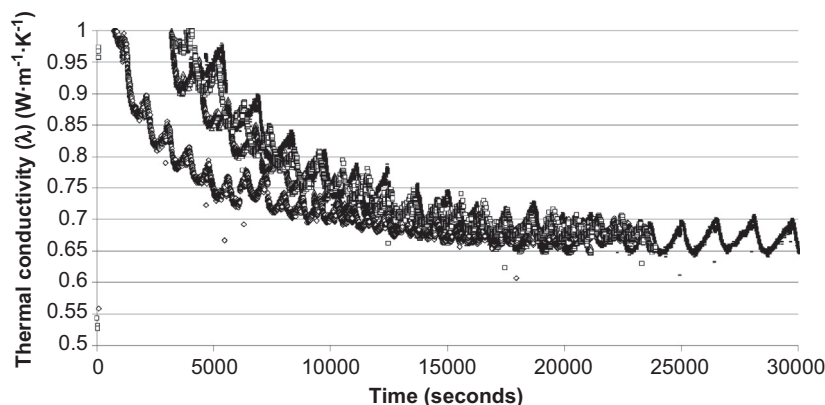


Fig. 9. Thermal conductivity vs time of the final sandwich panel at room temperature. Repeated cycles show the reproducibility of the obtained value.

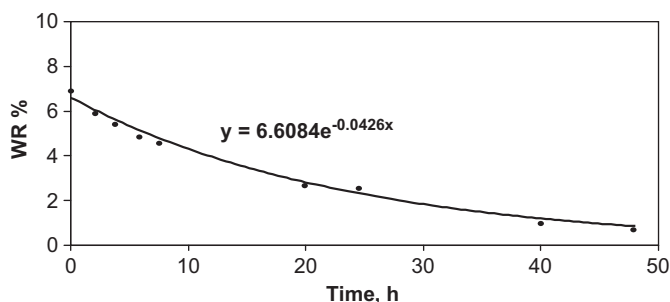


Fig. 10. Water release percentage plot  $WR_i$  (formula 3) versus time  $t_i$ .

#### 4. Conclusions

Alkali bonded ceramic composite panels with a sandwich structure were made by recycling up to 80 wt% of ceramic (porcelain stoneware) scraps.

An alkali-aluminosilicate binder (geopolymer) was used to perform a net shape-like consolidation at low temperature (80 °C).

Scraps proved to have their own surface reactivity toward geopolymerization, showing the way to further investigations on their potential reutilisation (in progress).

The thermal conductivity of the panels was 0.7 W m<sup>-1</sup> K<sup>-1</sup>, thus in the range of values of the so called thermal insulators.

Their high and fast water absorption and low water release make these panels suitable for cooling by water evaporation.

#### Acknowledgements

Thanks are due to Dr. M. Dondi, M. Raimondo and C. Zanelli for the useful scientific discussion and to Ms Samanta Fabbri for the samples preparation.

#### References

- [1] A. Juan, C. Medina, M.I. Guerra, J.M. Morán, P.J. Aguado, M.I. Sánchez de Rojas, M. Frías, O. Rodríguez, Re-use of ceramic wastes in construction, in: W. Wunderlich (Ed.), *Ceramic Materials*, InTech, 2010. pp 197–214.
- [2] A. Schwarz-Tatarin, S. Freyburg, Influence of scrap glass powders and the maturing process in the unfired state on the body properties of a kaolinitic clay after firing, *Journal of the European Ceramic Society* 30 (2010) 1619–1627.
- [3] E. Rambaldi, L. Esposito, A. Tucci, G. Timellini, Recycling of polishing porcelain stoneware residues in ceramic tiles, *Journal of the European Ceramic Society* 27 (2007) 3509–3515.
- [4] B. Huang, Q. Dong, E.G. Burdetteto, Laboratory evaluation of incorporating waste ceramic materials into Portland cement and asphaltic concrete, *Construction and Building Materials* 23 (2009) 3451–3456.
- [5] J. Davidovits, *Geopolymers Chemistry and Applications*, in: J. Davidovits (Ed.), Institut Geopolymere, Saint-Quentin, France, 2008.
- [6] W.M. Kriven, J.L. Bell, M. Gordon, Microstructure and microchemistry of fully-reacted geopolymers and geopolymer matrix composites, *Ceramic Transactions* 153 (2003) 227–250.
- [7] W.M. Kriven, M. Gordon, J. Bell, Geopolymers: nanoparticulate, nanoporous ceramics made under ambient conditions, in: I.M. Anderson, R. Price, E. Hall, E. Clark, S. McKernan, (Eds.), *Proceedings of the 62nd Annual Meeting of Microscopy Society of America*, Savannah: University of Cambridge, 2004, vol. 10, pp. 5–404.
- [8] A. Buchwald, M. Vicent, R. Kriegel, C. Kaps, M. Monzó, A. Barba, Geopolymeric binders with different fine fillers—phase transformations at high temperatures, *Applied Clay Science* 46 (2009) 190–195.
- [9] D.C. Comrie, W.M. Kriven, Composite cold ceramic geopolymer in a refractory application, *Ceramic Transactions* 153 (2003) 211–225.
- [10] Zhang Yunsheng, Sun Wei, Li Zongjin, Zhou Xiangming, Eddie, Chau Chungkong, Impact properties of geopolymer based extrudates incorporated with fly ash and PVA short fiber, *Construction and Building Materials* 22 (2008) 370–383.
- [11] Q. Zhao, B. Nair, T. Rahimian, P. Balaguru, Novel geopolymer based composites with enhanced ductility, *Journal of Materials Science* 42 (2007) 3131–3137.



- [12] T.S. Lin, D.C. Jia, P.G. He, M.R. Wang, D. Liang, Effects of fiber length on mechanical properties and fracture behaviour of short carbon fiber reinforced geopolymer matrix composites, *Materials Science and Engineering A* 497 (2008) 181–185.
- [13] K. Okada, A. Ooyama, T. Isobe, Y. Kameshima, A. Nakajima, K.J.D. MacKenzie, Water retention properties of porous geopolymers for use in cooling applications, *Journal of the European Ceramic Society* 29 (2009) 917–923.
- [14] C. Zanelli, M. Raimondo, G. Guarini, M. Dondi, The vitreous phase of porcelain stoneware: composition, evolution during sintering and physical properties, *Journal of Non-Crystalline Solids* 357 (2011) 3251–3260.
- [15] V. Medri, S. Fabbri, A. Ruffini, J. Dedeczek, A. Vaccari, SiC-based refractory paints prepared with alkali aluminosilicate binders, *Journal of the European Ceramic Society* 31 (2011) 2155–2165.
- [16] V. Medri, S. Fabbri, J. Dedeczek, Z. Sobalik, Z. Tvaruzkova, A. Vaccari, Role of the morphology and the dehydroxylation of metakaolins on geopolymerization, *Applied Clay Science* 50 (2010) 538–545.
- [17] J.L. Bell, P.E. Driemeyer, W.M. Kriven, Formation of ceramics from metakaolin-based geopolymers. Part II: K-based geopolymer, *Journal of the American Ceramic Society* 92 (2009) 607–615.
- [18] Z. Zuhua, Y. Xiao, Z. Huajun, C. Yue, Role of water in the synthesis of calcined kaolin-based geopolymer, *Applied Clay Science* 43 (2009) 218–223.
- [19] F. Frizon, C. Jousset Dubien, Method of Preparing a Controlled Porosity Geopolymer, the Resulting Geopolymer and the Various Applications Thereof. Patent Pub. N. US2010 0222204 A1, 2010.
- [20] E. Landi, V. Medri, E. Papa, J. Dedeczek, P. Klein, P. Benito and A. Vaccari, Alkali-bonded ceramics with hierarchical tailored porosity, *Applied Clay Science* 73, 2013, 56–64.
- [21] F. Zibouche, H. Kerdjoudj, J.-B. d'Espinose de Lacaillerie, H. Van Damme, Geopolymers from Algerian metakaolin. Influence of secondary minerals, *Applied Clay Science* 43 (2009) 453–458.
- [22] C. Panagiotopoulou, E. Kontori, T. Perraki, G. Kakali, Dissolution of aluminosilicate minerals and by-products in alkaline media, *Journal of Materials Science* 42 (2007) 2967–2973.
- [23] R.K. Iler, *The Chemistry of Silica*, John Wiley and Sons, New York, 1979.
- [24] V. Medri, A. Ruffini, Alkali-bonded SiC based foams, *Journal of the European Ceramic Society* 32 (2011) 1907–1913.
- [25] V. Medri, A. Ruffini, The influence of process parameters on in situ inorganic foaming of alkali-bonded SiC based foams, *Ceramics International* 38 (2011) 3351–3359.
- [26] E. Garcia, A. de Pablos, M.A. Bengoechea, L. Guaita, M.I. Osendi, P. Miranzo, Thermal conductivity studies on ceramic floor tiles, *Ceramics International* 37 (2011) 369–375.
- [27] P. Duxson, G.C. Lukey, J.S.J. van Deventer, Thermal conductivity of metakaolin geopolymers used as a first approximation for determining gel interconnectivity, *Industrial and Engineering Chemistry Research* 45 (2006) 7781–7788.
- [28] M. Raimondo, M. Dondi, D. Gardini, G. Guarini, F. Mazzanti, Predicting the initial rate of water absorption in clay bricks, *Construction and Building Materials* 23 (2009) 2623–2630.